Surface Science 652 (2016) 148–155

Contents lists available at ScienceDirect

Surface Science

journal homepage: www.elsevier.com/locate/susc

Temperature-programmed desorption study of NO reactions on rutile $TiO_2(110)$-1 × 1

Boseong Kim [a], Zdenek Dohnálek [b], János Szanyi [b], Bruce D. Kay [b], Yu Kwon Kim [a,*]

[a] Department of Energy Systems Research and Department of Chemistry, Ajou University, Suwon 443-749, South Korea
[b] Physical Sciences Division, Fundamental and Computational Sciences Directorate, Pacific Northwest National Laboratory, PO Box 999, Mail Stop K8-88, Richland, WA 99352, United States

ARTICLE INFO

Available online 24 February 2016

Keywords:
$TiO_2(110)$
Temperature-programmed desorption
Nitric oxide
Nitrogen dioxide
Nitrous oxide
NO dimers

ABSTRACT

Systematic temperature-programmed desorption (TPD) studies of NO adsorption and reactions on rutile $TiO_2(110)$-1 × 1 surface reveal several distinct reaction channels in a temperature range of 50–500 K. NO readily reacts on $TiO_2(110)$ to form N_2O, which desorbs between 50 and 200 K (LT N_2O channels), which leaves the TiO_2 surface populated with adsorbed oxygen atoms (O_a) as a by-product of N_2O formation. In addition, we observe simultaneous desorption peaks of NO and N_2O at 270 K (HT1 N_2O) and 400 K (HT2 N_2O), respectively, both of which are attributed to reaction-limited processes. No N-derived reaction product desorbs from $TiO_2(110)$ surface above 500 K or higher, while the surface may be populated with O_a's and oxidized products such as NO_2 and NO_3. The adsorbate-free TiO_2 surface with oxygen vacancies can be regenerated by prolonged annealing at 850 K or higher. Detailed analysis of the three N_2O desorption yields reveals that the surface species for the HT channels are likely to be various forms of NO dimers.

1. Introduction

As a part of the effort to reduce the NO_x emissions in combustion engines and power plants, a great deal of research has been invested in the design of efficient catalysts for the conversion of NO_x into nontoxic N_2 [1,2]. In this study, we aim to provide a fundamental level understanding of the underlying mechanism of catalytic reduction of NO [3–5] over TiO_2 catalysts. Such studies should provide a foundation for our understanding of the NO reduction over the TiO_2-based de-NO_x catalysts such as V_2O_5/TiO_2 [6,7], WO_3/TiO_2 [8], V_2O_5-WO_3/TiO_2 [9,10], and V_2O_5-MoO_3/TiO_2 [11].

A great deal of insight has been obtained from studies performed on model rutile $TiO_2(110)$ surfaces [12–16]. It has been shown that NO adsorbs molecularly below ~100 K and desorbs at 120 K [17]. Theoretical calculations revealed that NO binds to titanium sites with N atom with a binding energy of 8.4 kcal/mol [12]. A stronger binding energy of 35 kcal/mol on oxygen vacancy sites has been also predicted by theory. Further, other bonding configurations such as $(NO)_2$ dimers have been theoretically [12,15] predicted and recently observed experimentally [15,16].

In addition to molecular adsorption, the reactions of NO molecules adsorbed on $TiO_2(110)$ lead to the formation of N_2O, which desorbs in multiple peaks having temperatures of 170, 270, and 400 K [12,14,17]. Irradiation with photons can facilitate the reduction of molecularly adsorbed NO at low temperatures to initiate facile desorption of N_2O [13]. The oxygen atoms left behind, fill bridging oxygen vacancy (V_O's) defect sites effectively oxidizing the surface at the early stage of reaction [17]. According to our recent study [14], the surface charge associated with the V_O's strongly enhances the conversion of NO to N_2O at substrate temperatures as low as 50 K. A fraction of N_2O molecules desorb rapidly at 50 K while the rest can be liberated upon heating to ~180 K.

Although N_2O formation from NO has been observed on $TiO_2(110)$ in previous studies [12–14], the reaction mechanism appears complex and is far from being well-understood. This is clearly illustrated by complex N_2O desorption which exhibits several desorption channels peaking at 170, 270, and 400 K. Further, while the studies [17] performed on reduced $TiO_2(110)$ have shown that surface defects such as V_O's play an important role in NO reduction, the N_2O formation has been also observed on a fully oxidized [12] $TiO_2(110)$ with two desorption peaks at 170 and 250 K.

In this study, we focus on the coverage-dependent reactions of NO on pristine (*p*-TiO_2), reduced (*r*-TiO_2), hydroxylated (*h*-TiO_2), and oxidized TiO_2 (*o*-TiO_2). Our quantitative analysis of the N_2O desorption yields shows interesting details about the nature of the surface species responsible for the HT N_2O desorption channels.

2. Experimental details

The measurements were performed in an ultrahigh vacuum (UHV) molecular beam surface scattering apparatus with a base pressure of

* Corresponding author. Tel.: +82 31 219 2896; fax: +82 31 219 2969.
E-mail address: yukwonkim@ajou.ac.kr (Y.K. Kim).

http://dx.doi.org/10.1016/j.susc.2016.01.032
0039-6028/

1×10^{-10} torr equipped with quadrupole mass spectrometer (UTI-100C) that was described previously [18].

The rutile $TiO_2(110)$ substrate ($10 \times 10 \times 1$ mm^3, Princeton Scientific) was mounted on a Ta plate using a ceramic glue and a front retaining ring and its temperature was controlled between 50 and 1000 K [14]. The sample was cleaned by repeated Ne^+-ion sputtering and annealing to 870 K to prepare a well-ordered rutile $TiO_2(110)$-1×1 surface as determined from a sharp 1×1 pattern in low-energy electron diffraction (LEED). The concentration of bridging oxygen vacancies (V_O's) was monitored by measuring the area of the recombinative H_2O desorption peak at 500 K in temperature-programmed desorption (TPD) spectra [19–21]. At the early stages of this study (a small number of sputter–anneal cycles), the $TiO_2(110)$ crystal was transparent, exhibited a sharp 1×1 pattern in LEED, and the V_O concentration was negligible based on H_2O TPD. We refer to this *pristine* sample as *p*-TiO_2. With an increasing number (>10) of sputter–anneal cycles, the $TiO_2(110)$ crystal turned dark blue, and the V_O concentration increased to ~5% (~2.6×10^{13} cm^{-2}) (this sample is referred to as *r*-TiO_2). We have also prepared hydroxylated [22–24] and oxidized [25,26] $TiO_2(110)$ (referred to as *h*-TiO_2 and *o*-TiO_2, respectively). On *h*-TiO_2, the V_O defect sites have been reacted away by dosing 2 monolayers (ML) of H_2O on *r*-TiO_2 at 50 K followed by annealing to 400 K [19,25]. *o*-TiO_2 was prepared by oxidizing *r*-TiO_2 with molecular O_2 either by dosing ~2×10^{15} O_2/cm^2 at 300 K or by an O_2 dose of 1–5 $\times 10^{14}$ O_2/cm^2 at 50 K followed by annealing to 300 K [25,26].

Molecular NO was dosed using a neat NO beam (Matheson, CP Grade) at substrate temperatures between 50 and 100 K while recording mass fragments of possible reaction products such as N_2, N_2O, NO, and NO_2 using a quadrupole mass spectrometer (UTI 100C). The TPD spectra of NO and N_2 were determined by subtracting the contribution of the fragments of N_2O (m/z = 44 amu) from m/z = 30 (0.38 amu) and m/z = 28 (0.15 amu), respectively. The absolute N_2O coverage (in N_2O/cm^2) was obtained by comparing the integrated TPD area of the N_2O produced with the TPD spectra from a known amount of N_2O preadsorbed on TiO_2 [27]. The absolute NO dose (in NO/cm^2) was estimated from the plot of integrated area of NO TPD spectra obtained from multilayers of NO dosed on oxidized TiO_2 against the calibrated dose of NO by assuming that the sticking coefficient is unity at the dose temperature.

X-ray photoelectron spectroscopy (XPS) measurements were performed using a hemispherical analyzer (Omicron SPHERA 2000) and x-ray (Mg Kα) to confirm that no N species remained on the TiO_2 surface after a few cycles of TPD within detection limit of XPS.

3. Results and Discussion

Fig. 1 shows the TPD spectra of NO, N_2O, and N_2 desorbing after the NO adsorption on *p*-TiO_2 and *r*-TiO_2. We find that more NO (N_2O) desorbs from *p*-TiO_2 (*r*-TiO_2); that is, more N_2O is formed from NO on *r*-TiO_2, most likely due to the presence of V_O's [14]. Unreacted NO desorbs from both surfaces with TPD peaks at ~120 and 270 K and measurable desorption signal extending all the way to 400 K. N_2O, as a major reaction product, desorbs at a number of distinct desorption temperatures. The N_2O desorption at < 200 K is assigned to low-temperature (LT) N_2O. As shown in our previous study, N_2O forms readily even at temperatures as low as 50 K, and its formation is facilitated by the subsurface charge associated with V_O's [14]. On *r*-TiO_2, N_2O formed at the dose temperature may desorb from the surface or may remain physisorbed on the surface and contribute to the observed desorption peaks below 200 K [14].

In addition to the LT N_2O reaction channel, we also observe distinct N_2O desorption peaks at 270 and 400 K, labeled as high-temperature (HT) N_2O (HT N_2O). These HT N_2O TPD peaks are also accompanied by NO desorption. Since these desorption temperatures are much higher than the desorption temperatures of physisorbed NO and N_2O, the HT desorption peaks must result from reaction-limited desorption processes.

Fig. 1 also shows a clearly resolved desorption of N_2 at 250 K [14] in addition to N_2O desorption. The N_2 yield increases proportionally with NO dose up to ~1 ML whereupon it saturates at 0.7×10^{13} N_2/cm^2, corresponding to 3% of the NO dosed. The detailed mechanism of N_2 formation is not understood at this point, but the fact that the N_2 desorption temperature coincides with HT1 N_2O desorption suggests that the same surface species for HT1 N_2O formation is responsible for the reaction-limited N_2 formation.

NO TPD spectra following NO adsorption on *p*- and *r*-TiO_2 as a function of NO dose are shown in Fig. 2. The integrated amounts of desorbing NO are further plotted as a function of NO dose in the inset. At small NO

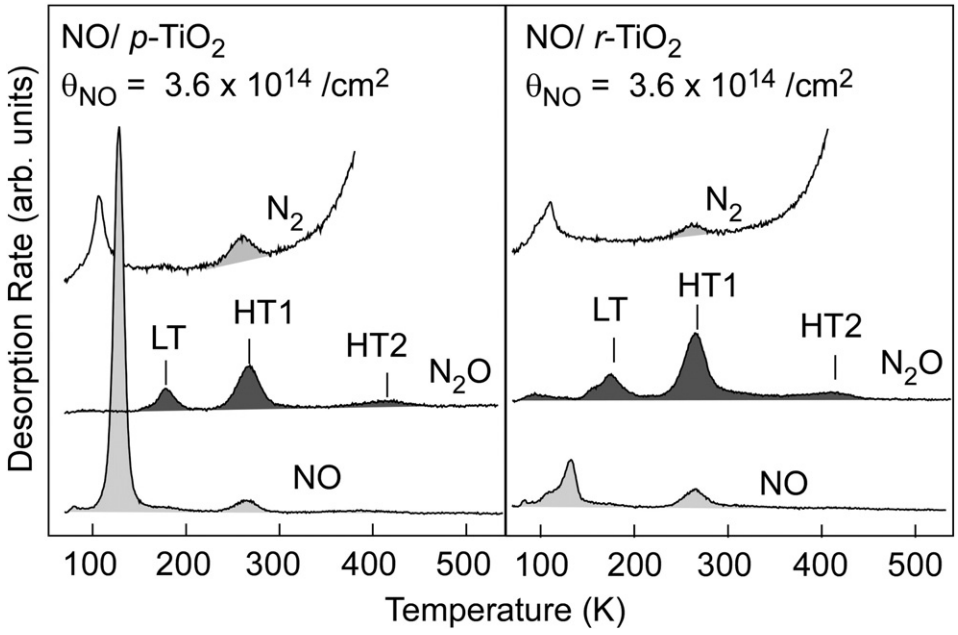

Fig. 1. NO, N_2O, and N_2 TPD spectra following NO adsorption ($\theta_{NO} = 3.6 \times 10^{14}$ NO/cm^2) on (a) *p*-TiO_2 (concentration of V_O's is <0.01 ML) and (b) *r*-TiO_2 (concentration of V_O's is 0.05 ML) at 50 K. The TPD spectra were acquired using a constant ramp rate of 1 K/s.

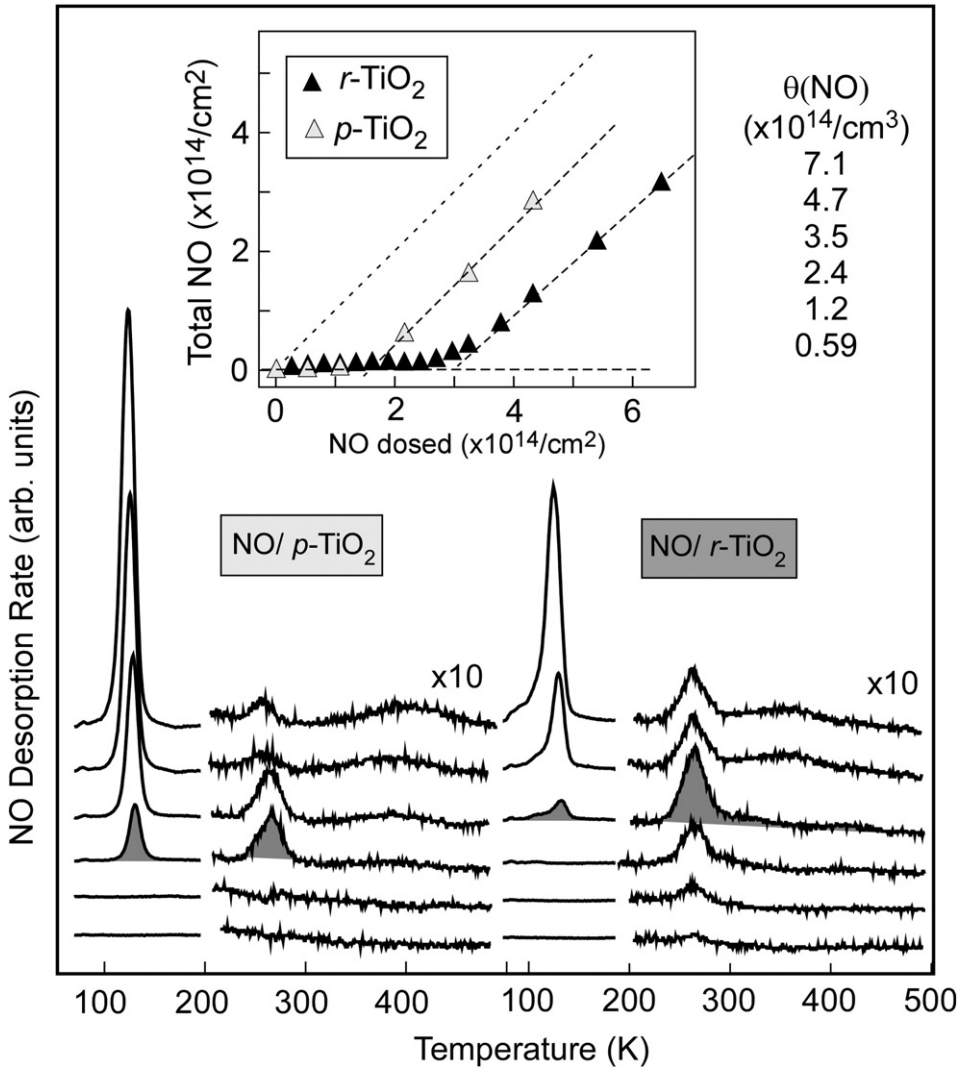

Fig. 2. NO TPD spectra from NO dosed on *p*- and *r*-TiO_2 as a function of NO dose. The inset shows the integrated amount of desorbing NO vs. NO dose. The number of Ti^{4+} sites on the surface is $5.2 \times 10^{14}/cm^2$ (≡1 ML).

doses (~1×10^{14} NO/cm^2), nearly all NO reacts to form products such as N_2O and NO_2. NO desorption is observed only above a certain threshold dose, which is 2.5×10^{14} NO/cm^2 for *r*-TiO_2 and 1×10^{14} NO/cm^2 for *p*-TiO_2. This result clearly shows that more NO reacts on *r*-TiO_2 than on *p*-TiO_2. Since the key difference between these two surfaces is the high concentration of V_O's (~5%) on *r*-TiO_2, the V_O's are attributed to the higher reactivity of *r*-TiO_2 than that of *p*-TiO_2 as has been observed from the role of V_O's in the enhanced LT N_2O formation yield [14].

Fig. 3 shows N_2O TPD spectra for different NO doses on *p*- and *r*-TiO_2. On both surfaces, the HT1 N_2O peak initially increases, maximizes at NO dose of ~3.5×10^{14} NO/cm^2 and subsequently decreases at higher NO doses. The HT2 N_2O peak is relatively small but shows a similar NO dose-dependent trend as the HT1 N_2O desorption peak. By contrast, the LT N_2O peak increases proportionally with the NO dose. A comparison of the N_2O spectra from *r*- and *p*-TiO_2 reveals that the trends are very similar except that the overall N_2O desorption yield is higher on *r*-TiO_2 at higher NO doses.

At low NO doses, the intensity of N_2O desorption peaks from *p*-TiO_2 is slightly higher than that from *r*-TiO_2. Since more N_2O desorption occurs during the NO dose on *r*-TiO_2, it is likely that more oxygen adatoms are left on the *r*-TiO_2 at the low NO dose regime. It may facilitate the formation of further oxidized forms of NO such as NO_2 and NO_3 better on *r*-TiO_2 than on *p*-TiO_2. This may act as a factor of suppressing the yield of the reductive channel (N_2O desorption) on *r*-TiO_2 than on *p*-TiO_2 at the low NO dose regime.

The integrated N_2O amounts observed in three observed N_2O TPD peaks (LT, HT1, and HT2) as well as the total N_2O from both *r*-TiO_2 and *p*-TiO_2 are plotted against the NO dose in Fig. 4. Several interesting features can be observed in the NO coverage-dependent trends of N_2O desorption yield. First, the total N_2O yield increases up to the NO dose of 2.5×10^{14} and 4×10^{14} NO/cm^2 on *p*- and *r*-TiO_2, respectively, then saturates at higher doses. The total N_2O yield from *r*-TiO_2 is higher than that from *p*-TiO_2 by ~$3.5 \times 10^{13}/cm^2$. This can be attributed to the presence of V_O's on *r*-TiO_2. The V_O's also lead to the N_2O desorption below 100 K from NO dosed on *r*-TiO_2(110) [14]. Some of N_2O formed at the dose temperature is physisorbed and desorbs below 200 K during the TPD ramp. N_2O may be also formed during the ramp as the molecularly bound NO species diffuse on the surface and react with each other forming $N_2O + O_a$ at low temperatures (up to 120 K). These possible channels contribute to LT N_2O desorption below 200 K.

Second, the HT1 N_2O yield does not saturate, but decreases at higher NO doses. The maximum yield of HT1 N_2O is reached at the NO dose of 2.5×10^{14} and 3.5×10^{14} NO/cm^2 on *p*- and *r*-TiO_2, respectively, which decreases as the NO dose increases further. The loss in HT1 N_2O yield is largely compensated by an increase in the LT N_2O yield; this results in a saturation in the total N_2O yield for both *r*- and *p*-TiO_2. As the NO dose

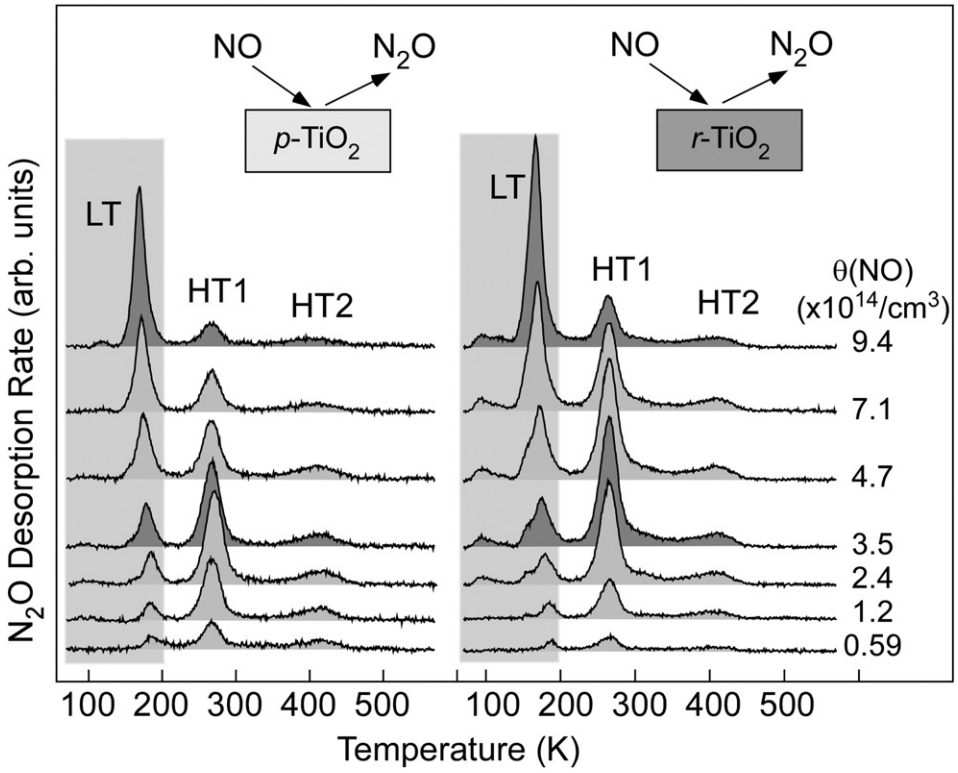

Fig. 3. TPD spectra of N_2O desorption from NO dosed on two different TiO_2 surfaces (p-TiO_2 and r-TiO_2) with increasing NO dose.

increases to a saturation of monolayer, the increased NO–NO interaction may facilitate the formation of N_2O at lower temperatures (<200 K); it may limit the formation of the surface NO-derived species responsible for the HT N_2O such as stable forms of NO dimers. The absolute yield for the HT2 N_2O is low, but the NO dose-dependent trend follows a similar trend as HT1.

Third, there is a deficiency between the NO dose and the sum of NO and N_2O desorption yields. For example, for the NO dose of 3.5×10^{14} NO/cm^2 on r-TiO_2, the total N_2O yield is ~8×10^{13} N_2O/cm^2, and the amount of unreacted NO desorption is about 5×10^{13} NO/cm^2. After adding the N_2O desorption during the NO dose (~1×10^{13} N_2O/cm^2), the total N_2O yield equals to ~9×10^{13} N_2O/cm^2 accounting for the NO dose of 1.8×10^{14} NO/cm^2. The desorbing amounts of NO and N_2O account for 2.3×10^{14} NO/cm^2. Thus, a significant fraction of NO (~1.2×10^{14} NO/cm^2) remains unaccounted. This discrepancy is larger than that expected from a possible calibration error (~10–20%), which leads us to conclude that there are N species that are not desorbed from the surface during TPD up to about 650 K. It is likely that oxidized species such as NO_2 and NO_3 are left on the surface. We cannot detect further desorption of any N-related species above 500 K up to 850 K. In addition, XPS measurements carried out after the NO TPD up to 200–500 K sometimes show noisy signals at 400–406 eV only at the first scan, which quickly disappear at the subsequent scans, resulting in no meaning features of N 1s spectra. We believe that this is because

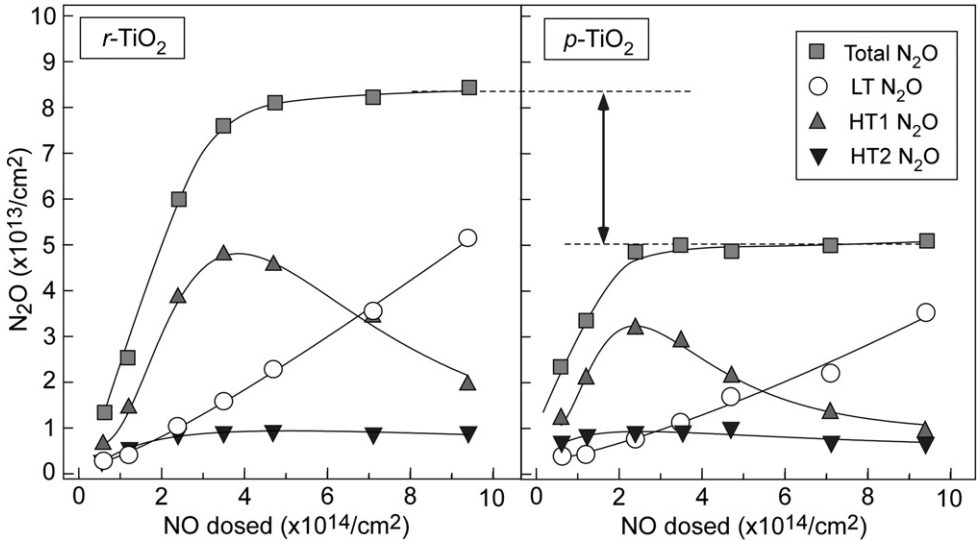

Fig. 4. The integrated amounts of N_2O for the three different channels, LT, HT1, and HT2 as well as that of total N_2O obtained from TPD peaks in Fig. 3 as a function of NO dose on p- and r-TiO_2.

such NO_2 and NO_3 species are very unstable under x-ray irradiation in a UHV condition. Thus, we speculate that they are oxidized forms of NO such as NO_2 and NO_3, which can be produced by reactions of NO with oxygen adatoms.

However, a small measurable amount of stable N species is found from XPS after several cycles of NO TPD (>10 cycles). This fact also supports the idea that there are surface N species left from NO reactions on TiO_2, in oxidized forms such as NO_2 and NO_3; several cycles of TPD may induce the formation of stable NO_3 aggregates instead of the isolated NO_3.

A strong correlation between V_O's on *r*-TiO_2 and the NO reactivity is further corroborated from Fig. 5. It shows H_2O TPD obtained after NO TPD up to 400 K at various NO doses. After the NO TPD, H_2O is dosed to probe the V_O sites that remain following the NO adsorption and reactions. The same method has been used to determine the concentration of V_O's on bare *r*-TiO_2 surfaces as described in the experimental section [19,21,25]. The H_2O TPD spectra in Fig. 5 show that the recombinative H_2O desorption peak at 500 K ($2OH_b \rightarrow H_2O(g) + O_b + V_O$) decreases significantly already at very low NO doses ($<5 \times 10^{13}$ NO/cm^2). The dependence of the integral of the recombinative H_2O TPD peak on the NO dose is shown in the upper inset of Fig. 5. The observed dependence shows that the V_O concentration decreases quite in proportion to the NO dose and that it is reduced to one third of the initial value (2.6×10^{13} V_O/cm^2) at ~5×10^{13} NO/cm^2. We speculate that this is the result of V_O's being preferentially filled with oxygen atoms left behind from the N_2O formation from NO [14].

Considering that the formation of N_2O from NO leaves O_a on TiO_2(110), the effect of predosed oxygen on the reactivity of NO is investigated in Fig. 6. The figure shows the TPD spectra of NO and N_2O from NO dosed on O_2-predosed *r*-TiO_2 at fixed NO dose ($\theta_{NO} = 3.5 \times 10^{14}$ NO/cm^2), while the O_2 dose is increased up to 3.5×10^{14}/cm^2. NO TPD (left) shows that the LT NO desorption increases with increasing O_2, suggesting that the reactivity of NO over TiO_2 decreases due to the effect of predosed O_2. As a result, unreacted NO contributes to the increase of NO desorption yield with increasing O_2 dose as quantified in the left inset of Fig. 6. The TPD spectra of N_2O (right) show that the total N_2O desorption yield decreases with increasing O_2 doses.

The N_2O desorption yield from different channels is shown in the upper right inset of Fig. 6. Note that the decrease of HT1 N_2O yield is more pronounced than that of LT N_2O. As the predosed O_2 increases, the HT1 N_2O yield vanishes at an O_2 dose of ~2×10^{14} O_2/cm^2, while

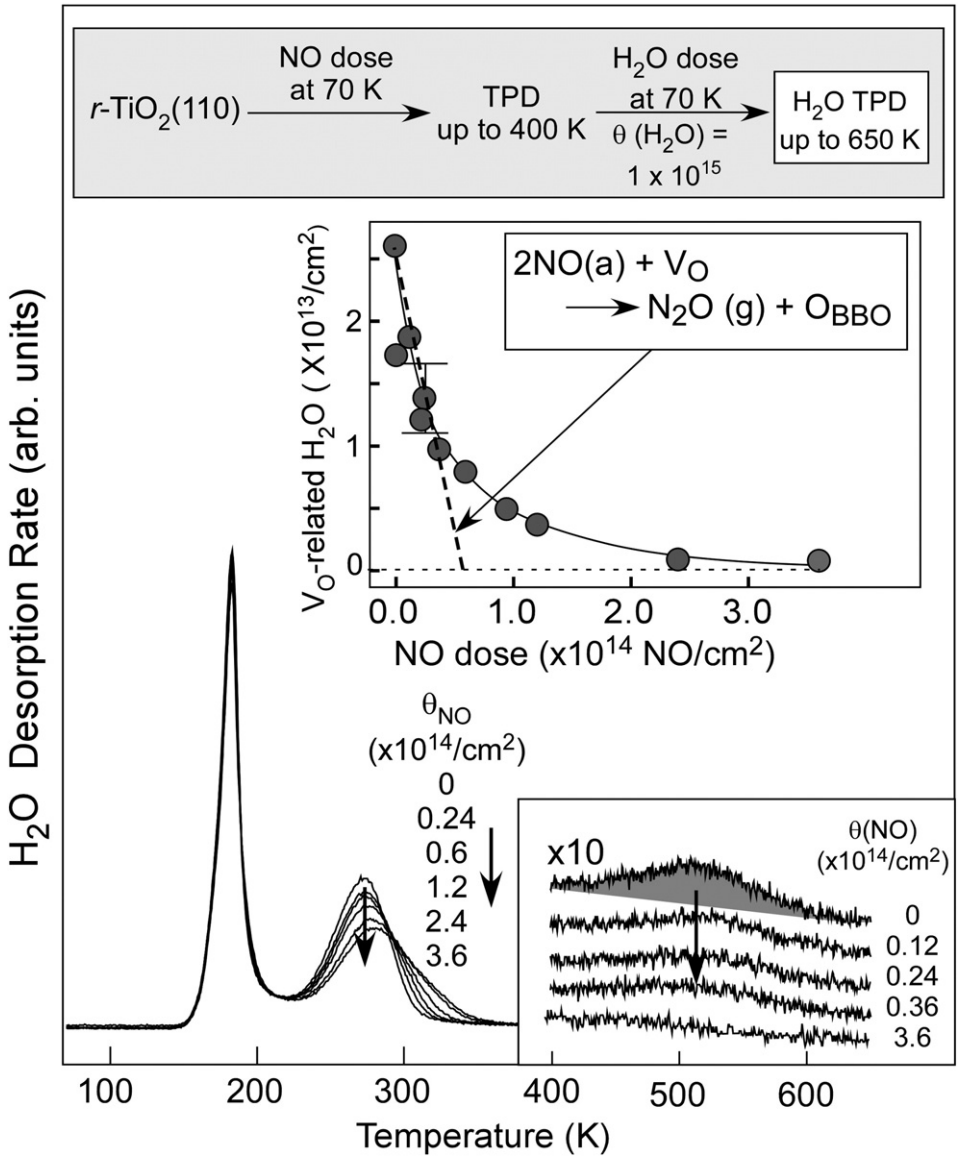

Fig. 5. H_2O TPD (dose = 1×10^{15} H_2O/cm^2) from *r*-TiO_2 after dosing different amounts of NO at 70 K and TPD to 400 K. The recombinative H_2O desorption at 500 K (bottom inset) from available V_O sites shows that V_O's are readily depleted as a result of NO adsorption and reaction.

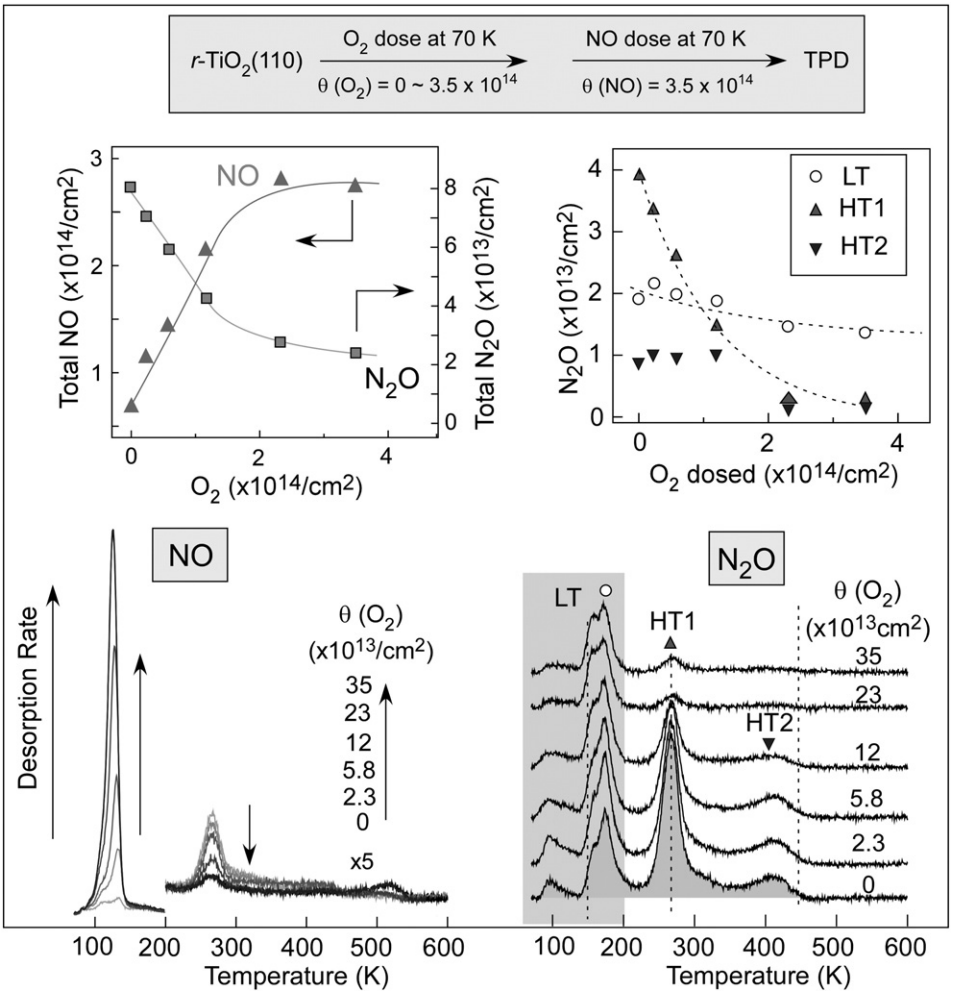

Fig 6. TPD spectra showing NO (left) and N_2O (right) desorption from NO dosed on O_2-predosed *r*-TiO_2. The insets show the total NO (top left) and N_2O (top right) yields for various N_2O desorption channels plotted as a function of the O_2 dose.

the LT N_2O yield persists. Thus, the formation of surface NO-derived species responsible for the HT N_2O is more likely to be suppressed by the presence of predosed O_2 probably via the depletion of surface charge associated with oxygen vacancies. The predosed O_2 may fill the oxygen vacancies which can otherwise act as a binding site for NO dimers, e.g., $(NO)_2^-$. The NO dimer ($(NO)_2^-$) can be a likely candidate for HT1 N_2O peak since the decomposition of the dimer into N_2O and O_a at ~270 K can readily induce desorption of N_2O (reaction-limited desorption).

The LT N_2O yield is also suppressed slightly but still shows a significant desorption yield of ~1.5×10^{13} N_2O/cm^2 even at 3.5×10^{14} O_2/cm^2. Despite the persistent nature of the LT N_2O yield, we have also seen that during the NO dose on *r*-TiO_2, the LT N_2O desorption at the dose temperature (~50 K) is also strongly influenced by the depletion of surface charges by predosed O_2 [14]. In Fig. 6, NO is subsequently dosed following the O_2 dose at the low temperature and the TiO_2 is not fully oxidized under the condition. It is attributed to the origin of the persistent LT N_2O yield.

The effect of oxygen on the N_2O desorption channels is further studied by comparing N_2O TPD spectra taken from NO dosed on two different TiO_2 surfaces of *o*-TiO_2 and *r*-TiO_2, respectively. On *o*-TiO_2 (Fig. 7(a)), LT N_2O desorption is observed only above 4×10^{14} NO/cm^2; no HT N_2O desorption is observed throughout the whole NO doses up to 1×10^{15} NO/cm^2. This is consistent with earlier observations of Sorescu *et al.* on N_2O desorption from oxidized TiO_2(110) [12]. We can speculate that the formation of possible surface precursors (e.g., NO dimers) for the HT N_2O desorption channels is inhibited as a result of the depletion of V_O's (as well as surface charges associated with them).

Fig. 8 shows the behavior of the HT N_2O desorption channels when the surface is hydroxylated (*h*-TiO_2). Fig. 8(a) compares N_2O TPD spectra taken from three different TiO_2 surfaces: *r*-TiO_2, *h*-TiO_2, and H_2O predosed *h*-TiO_2. Note that the HT1 N_2O desorption peak is significantly reduced on *h*-TiO_2 compared to *r*-TiO_2, while the LT and HT2 N_2O desorption peaks are greatly enhanced. The HT1 N_2O is nearly depleted when a small amount of H_2O (~2×10^{13} H_2O/cm^2) is predosed on the *h*-TiO_2. The quantitative evaluation on the three N_2O yields is displayed in Fig. 8(b). The sum of N_2O on *h*-TiO_2 is slightly lower than that on *r*-TiO_2 by ~0.5×10^{13} N_2O/cm^2 due to the formation of NH_3 from the reaction between HO_b's and NO [28].

The data presented above imply that the presence of hydroxyls (and water) can deplete the surface species (probably $(NO)_2^-$) that lead to the HT1 N_2O desorption channel. Despite the quenching of the HT1 N_2O channel, the total N_2O yield does not vary much over the three TiO_2 surfaces. Recent STM studies performed at RT [29] show that the adsorbed NO is stabilized next to the hydroxyl species. We speculate that the low-temperature NO adsorption can possibly also yield more stable $(NO)_2^-$ dimers on *h*-TiO_2 than on *r*-TiO_2. Such species can be a source of the HT2 N_2O desorption that is observed on *h*-TiO_2.

Oxidized NO species such as NO_2 may be further oxidized by H_2O to make nitrate (NO_3) as has been reported earlier on oxide surfaces [30], including TiO_2 [31]. HO_b's on *h*-TiO_2 may react with O_a's to form OH_t's on the Ti^{4+} rows on the TiO_2(110) surface [32], subsequently forming H_2O

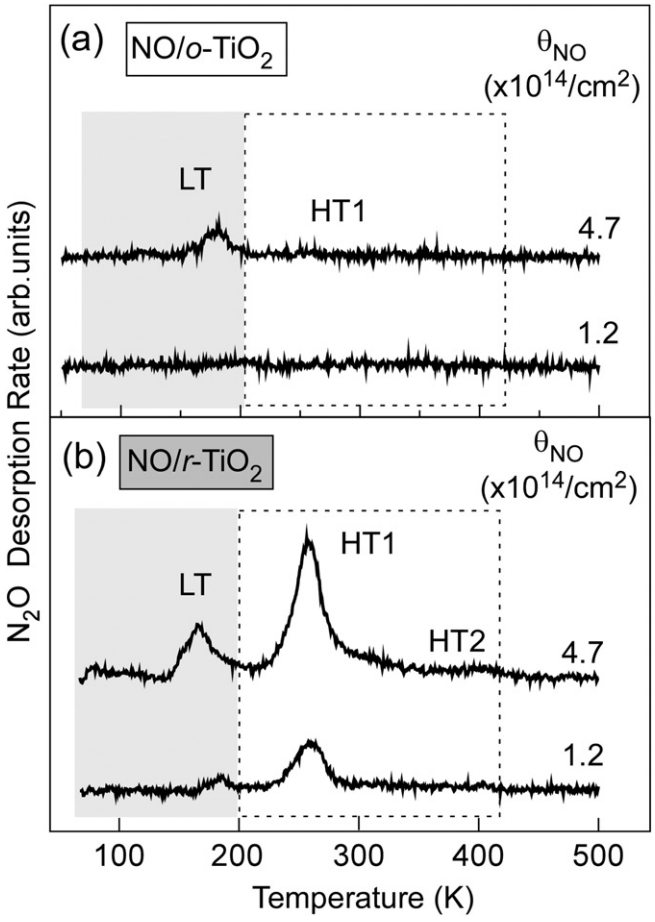

Fig. 7. Comparison of TPD spectra of N_2O desorbing from NO dosed on (a) *o*-TiO_2 and (b) *r*-TiO_2, respectively.

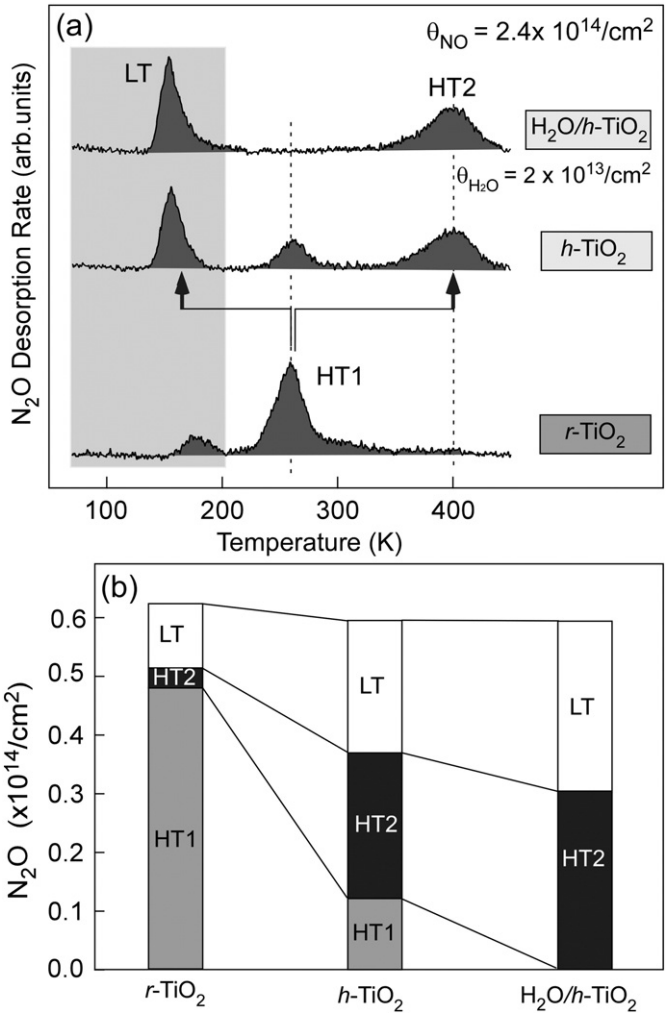

Fig. 8. (a) Comparison of TPD spectra of N_2O desorbing from NO (NO dose = 2.4×10^{14} NO/cm^2) dosed on *r*-TiO_2, *h*-TiO_2, and H_2O/*h*-TiO_2, respectively. It shows an intensity variation of each N_2O desorption channel on three different TiO_2 surfaces. (b) The N_2O desorption yields of LT, HT1, and HT2 channels compared for three different substrates of *r*-TiO_2, *h*-TiO_2, and H_2O predosed *h*-TiO_2. NO dose is fixed to 2.4×10^{14} NO/cm^2.

which desorbs at 300–400 K. Coadsorbed H_2O also interacts with O_a to form OH_t's [33]. Such OH_t species may react with NO_2 to form HNO_3, which can dissociate into H^+ and NO_3^- on TiO_2. However, this process is not likely to change the total N_2O yield as long as NO_2 and NO_3 do not contribute to the N_2O desorption channels.

The presence of hydroxyls also enhances the formation of LT N_2O (Fig. 8). The detailed mechanism for the enhanced LT N_2O desorption on *h*-TiO_2 is unclear, but we speculate that the presence of hydroxyls (and water) may also stabilize the adsorbed NO toward LT N_2O formation channel, probably via NO dimers.

We postulate that possible candidates for surface species responsible for the HT N_2O desorption channels can be NO dimers (e.g., $(NO)_2^-$) and hydroxyl-stabilized NO dimers for HT1 and HT2 N_2O, respectively. NO reduction on metal surfaces such as Ag [34,35], Au [36], Cu [37], and Pd [38] is proposed to involve $(NO)_2$ dimers as intermediates. In addition, such coupled NO species in the form of hyponitrite $(N_2O_2)^{2-}$ are also proposed as the intermediates of NO reduction cycles in biological systems employing NO reductase (NOR) [39] and flavodiiron NO reductase (FDP) [40].

NO dimers of various forms (e.g., cis and trans) have been proposed to have binding energies of 10–15 kcal/mol theoretically [12,41], which vary depending on the bonding configuration; they are suggested to decompose into $N_2O(a)$ and O_a below 200 K according to a recent FTIR study [41]. However, charged $(NO)_2^{2-}$ species may survive above 200 K and possibly contribute to HT1 N_2O desorption as previously observed for NO reactions on MnO_x/CeO_2 at 295 K [42]. In addition, bonding configuration of the NO dimers such as cis or trans can determine the energy barrier toward N_2O formation [43], which may give rise to N_2O desorption at different temperatures. Then, the observed variation in N_2O desorption channels above the threshold NO dose in Fig. 4 may be the result of varying ratio between different bonding configurations (e.g., cis and trans) with increasing NO doses. At low NO coverages the formation of trans-hyponitrites are favored and N_2O desorption is observed in the HT1 state primarily. As the surface becomes more crowded at higher NO exposures, the formation of cis-hyponitrites is prevalent. Since the decomposition of cis-hyponitrites is energetically less demanding than that of the trans conformer, N_2O desorption is observed in the LT state as the NO exposure increases.

NO_2 has been suggested to be formed from NO dosed on TiO_2(110) both experimentally and theoretically [15,16]. Theoretical studies [15,44] on NO_2/TiO_2 indicate that NO_2 is more strongly bound to TiO_2 than NO when NO_2 is bound to the Ti sites with its two oxygen atoms (η^2-bonding configuration). NO_2 may be further oxidized to NO_3 species, which are likely to survive above 400 K [31,44], too. The formation of oxidized species such as NO_2 and NO_3 on the surface is suggested to be the origin of the discrepancy in the total amount of NO dosed and that desorbed in Fig. 4.

4. Conclusions

A systematic temperature-programmed desorption (TPD) study of NO reactions with rutile TiO_2(110) surface has been performed. Low-

temperature (<200 K, LT N_2O), desorption-limited, and high-temperature (>200 K, HT N_2O) reaction-limited N_2O formation channels are observed in the TPD spectra. The insight obtained from these results is summarized below.

(i) The LT N_2O desorption channel increases approximately linearly on reduced TiO_2(110) (r-TiO_2) with increasing NO coverages. The branching into this channel is strongly reduced in the absence of surface charge associated with bridging oxygen vacancies (V_O's) as evident from the comparison of NO reactivity on r-TiO_2 and o-TiO_2 (TiO_2(110) surface oxidized by O_2).

(ii) The HT N_2O yield exhibits a maximum at intermediate NO doses but decreases as the NO dose is increased further. The maximum yield is obtained at a NO dose of 3.5×10^{14} and 2.5×10^{14} NO/cm^2 for r-TiO_2 and p-TiO_2 (TiO_2(110) with negligible V_O coverage). The observed HT N_2O decrease is correlated with increased LT N_2O formation; this results in a saturation in the overall N_2O yield above the intermediate NO dose.

(iii) The higher HT N_2O yield on r-TiO_2 as compared to p-TiO_2 indicates the importance of V_O's (and surface charges associated with them) in the formation of surface species responsible for the HT channel. The importance of surface charge is further supported by suppression of the HT N_2O desorption channel in the presence of the predosed oxygen.

(iv) There are also reaction-limited N_2 and NO desorption peaks at the same temperature as the HT1 N_2O desorption, which may be attributed to the competition between the three competing reaction channels originating from the same surface species.

(v) The HT2 N_2O desorption channel (along with the LT N_2O channel) is enhanced in the presence of hydroxyls (h-TiO_2), while the HT1 N_2O desorption channel is reduced. The suppression of the HT1 N_2O channel and the appearance of a new HT2 N_2O channel on h-TiO_2 is likely the result of stabilization of NO (dimers) in the presence of hydroxyls.

(vi) The discrepancy between the amount of NO dosed and that desorbed exists; it is likely the result of formation of oxidized species such as NO_2 and NO_3.

Acknowledgments

Y. K. Kim acknowledges financial support from the Basic Science Research Program through the National Research Foundation of Korea (NRF) funded by the Ministry of Education, Science and Technology (NRF-2012R1A1A2007641). ZD, JS, and BDK were supported by the US Department of Energy, Office of Science, Office of Basic Energy Sciences, Division of Chemical Sciences, Geosciences and Biosciences. The research was performed using EMSL, a national scientific user facility sponsored by the Department of Energy's Office of Biological and Environmental Research and located at Pacific Northwest National Laboratory (PNNL). PNNL is a multiprogram national laboratory operated for the DOE by Battelle.

References

[1] Z. Liu, S. Ihl Woo, Catal. Rev. 48 (2006) 43.
[2] P. Forzatti, Appl. Catal., A 222 (2001) 221.
[3] G. Busca, M.A. Larrubia, L. Arrighi, G. Ramis, Catal. Today 107–108 (2005) 139.
[4] V.I. Pârvulescu, P. Grange, B. Delmon, Catal. Today 46 (1998) 233.
[5] F. Garin, Appl. Catal., A 222 (2001) 183.
[6] G.T. Went, L.-J. Leu, R.R. Rosin, A.T. Bell, J. Catal. 134 (1992) 492.
[7] S.B. Kristensen, A.J. Kunov-Kruse, A. Riisager, S.B. Rasmussen, R. Fehrmann, J. Catal. 284 (2011) 60.
[8] H. Zhang, J. Han, X. Niu, X. Han, G. Wei, W. Han, J. Mol. Catal. A 350 (2011) 35.
[9] L. Lietti, J.L. Alemany, P. Forzatti, G. Busca, G. Ramis, E. Giamello, F. Bregani, Catal. Today 29 (1996) 143.
[10] P.G.W.A. Kompio, A. Brückner, F. Hipler, G. Auer, E. Löffler, W. Grünert, J. Catal. 286 (2012) 237.
[11] L. Lietti, I. Nova, G. Ramis, L. Dall'Acqua, G. Busca, E. Giamello, P. Forzatti, F. Bregani, J. Catal. 187 (1999) 419.
[12] D.C. Sorescu, C.N. Rusu, J.T. Yates, J. Phys. Chem. B 104 (2000) 4408.
[13] C.N. Rusu, J.T. Yates, J. Phys. Chem. B 104 (2000) 1729.
[14] B. Kim, Z. Li, B.D. Kay, Z. Dohnálek, Y.K. Kim, J. Phys. Chem. C 118 (2014) 9544.
[15] D. Stodt, H. Noei, C. Hattig, Y. Wang, Phys. Chem. Chem. Phys. 15 (2013) 466.
[16] M. Xu, Y. Wang, S. Hu, R. Xu, Y. Cao, S. Yan, Phys. Chem. Chem. Phys. 16 (2014) 14682.
[17] G. Lu, A. Linsebigler, J.T. Yates, J. Phys. Chem. 98 (1994) 11733.
[18] Z. Dohnálek, J. Kim, O. Bondarchuk, J. Mike White, B.D. Kay, J. Phys. Chem. B 110 (2006) 6229.
[19] M.A. Henderson, Langmuir 12 (1996) 5093.
[20] Y.K. Kim, B.D. Kay, J.M. White, Z. Dohnálek, J. Phys. Chem. C 111 (2007) 18236.
[21] M.A. Henderson, Surf. Sci. 400 (1998) 203.
[22] S. Wendt, P.T. Sprunger, E. Lira, G.K.H. Madsen, Z. Li, J.Ø. Hansen, J. Matthiesen, A. Blekinge-Rasmussen, E. Lægsgaard, B. Hammer, F. Besenbacher, Science 320 (2008) 1755.
[23] C.M. Yim, C.L. Pang, G. Thornton, Phys. Rev. Lett. 104 (2010) 036806.
[24] A.C. Papageorgiou, N.S. Beglitis, C.L. Pang, G. Teobaldi, G. Cabailh, Q. Chen, A.J. Fisher, W.A. Hofer, G. Thornton, Proc. Natl. Acad. Sci. 107 (2010) 2391.
[25] Z. Dohnálek, I. Lyubinetsky, R. Rousseau, Prog. Surf. Sci. 85 (2010) 161.
[26] M.A. Henderson, W.S. Epling, C.L. Perkins, C.H.F. Peden, U. Diebold, J. Phys. Chem. B 103 (1999) 5328.
[27] B. Kim, Z. Li, B.D. Kay, Z. Dohnalek, Y.K. Kim, J. Phys. Chem. C 116 (2012) 1145.
[28] B. Kim, B.D. Kay, Z. Dohnálek, Y.K. Kim, J. Phys. Chem. C 119 (2015) 1130.
[29] S.-C. Li, P. Jacobson, S.-L. Zhao, X.-Q. Gong, U. Diebold, J. Phys. Chem. C 116 (2012) 1887.
[30] B.J. Finlayson-Pitts, L.M. Wingen, A.L. Sumner, D. Syomin, K.A. Ramazan, Phys. Chem. Chem. Phys. 5 (2003) 223.
[31] J. Haubrich, R.G. Quiller, L. Benz, Z. Liu, C.M. Friend, Langmuir 26 (2010) 2445.
[32] Z. Zhang, Y. Du, N.G. Petrik, G.A. Kimmel, I. Lyubinetsky, Z. Dohnálek, J. Phys. Chem. C 113 (2009) 1908.
[33] Y. Du, N.A. Deskins, Z. Zhang, Z. Dohnalek, M. Dupuis, I. Lyubinetsky, Phys. Rev. Lett. 102 (2009) 096102.
[34] Z.-P. Liu, S.J. Jenkins, D.A. King, J. Am. Chem. Soc. 126 (2004) 7336.
[35] W.A. Brown, D.A. King, J. Phys. Chem. B 104 (2000) 2578.
[36] Z. Wu, L. Xu, W. Zhang, Y. Ma, Q. Yuan, Y. Jin, J. Yang, W. Huang, J. Catal. 304 (2013) 112.
[37] A. Shiotari, Y. Kitaguchi, H. Okuyama, S. Hatta, T. Aruga, Phys. Rev. Lett. 106 (2011) 156104.
[38] L.-y. Huai, C.-z. He, H. Wang, H. Wen, W.-c. Yi, J.-y. Liu, J. Catal. 322 (2015) 73.
[39] J. Wang, M.P. Schopfer, S.C. Puiu, A.A.N. Sarjeant, K.D. Karlin, Inorg. Chem. 49 (2010) 1404.
[40] T. Hayashi, J.D. Caranto, D.A. Wampler, D.M. Kurtz, P. Moënne-Loccoz, Biochemistry 49 (2010) 7040.
[41] Y. Wang, R. Kováčik, B. Meyer, K. Kotsis, D. Stodt, V. Staemmler, H. Qiu, F. Traeger, D. Langenberg, M. Muhler, C. Wöll, Angew. Chem. 46 (2007) 5624.
[42] J. Szanyi, J.H. Kwak, Chem. Commun. 50 (2014) 14998.
[43] A.M. Wright, T.W. Hayton, Inorg. Chem. 54 (2015) 9330.
[44] J.A. Rodriguez, T. Jirsak, G. Liu, J. Hrbek, J. Dvorak, A. Maiti, J. Am. Chem. Soc. 123 (2001) 9597.